# Tunneling Current of an AlGaAs/GaAs Multiple-quantum-well Solar Cell Considering a Trapezoidal Potential Barrier

Avigyan Chatterjee*‡, Sayantan Biswas* and Amitabha Sinha*

*Department of Physics, University of Kalyani, Kalyani-741235, West Bengal, India.

(avigyan.chatterjee@gmail.com, sayan.solar@gmail.com, asinha333@gmail.com)

‡Corresponding Author; Avigyan Chatterjee, Department of Physics, University of Kalyani, Kalyani-741235, West Bengal, India.

(avigyan.chatterjee@gmail.com)

Mob. No. : +918902229025

**Abstract:** The barrier created in the intrinsic multiple quantum well (MQW) region of a quantum well solar cell (QWSC) appears to be trapezoidal in nature. Therefore, in this paper, a trapezoidal barrier has been considered and the expression for the tunneling current of the QWSC has been obtained. The variation of the tunneling current with temperature has been shown graphically. In addition to this, the expressions for temperature and wavelength dependent refractive indices of different regions of the QWSC have been taken into account while performing the calculations of reflection coefficient. It has been shown in this paper graphically that QWSC with ZnS antireflection coating shows better performance than the cell without antireflection coating. Solar cells having different well width and barrier width have been chosen and the variation of the tunneling current densities with wavelength of incident light and temperature of the device has been studied for each cell. It has been observed that the tunneling current density falls with increase in the temperature of the cell.

## 1. Introduction

It is a very well known fact that with the tremendous development of science and technology the requirement of energy has been increased drastically. The main source of energy till now is fossil fuels like coal, natural gas, natural oil etc. But these sources are limited and pollute the environment. So we need alternative sources of energy. Different types of research and development works have already been done on the alternative sources of energy [1-6]. Solar cell is an alternative source of energy which does not create any kind of pollution. During the last few years various research works have been performed by several researchers on the high efficiency solar cells [7-9]. Quantum well solar cell is one of the members of the high efficiency solar cell family. Quantum tunneling is one of the most interesting phenomena in quantum mechanics and it plays a vital role in the generation of current in a quantum well solar cell (QWSC). QWSCs have been studied extensively during

the last two decades. Sequential resonant tunneling to enhance the photocurrent and reduce the recombination losses in photovoltaic devices based on multiple-quantum-well (MQW) heterostructures has already been proposed [10]. A brief review of the experimental and theoretical studies of QWSCs has been given including a number of theoretical models for such cells [11]. The impact of quantum effects on the absorption and tunneling current as a function of electric fields and light trapping ratios have been calculated and it has been shown that increasing electric fields enhance tunneling of photo-generated carriers, which dominates over the opposing effect of reduced absorption [12]. Aperathitis et al. [13] have shown experimentally the temperature dependence of the photocurrent in AlGaAs/GaAs MQW solar cells and have theoretically discussed three types of current components in the MQW solar cells, namely the tunneling current, thermionic current and photo-generated current assuming a rectangular potential

barrier. Again, assuming rectangular potential barriers, Chatterjee et al.[14] have extended the work of Aperathitis and have shown theoretically the temperature dependence of the three current components as mentioned above. In this paper, a trapezoidal potential barrier has been assumed and the expressions for the tunneling current of the solar cell have been obtained. Based on this analysis, the temperature dependence and wavelength dependence of the tunneling current density of the solar cell has been computed. It is also

observed that the total photo-current is consistent with the experimental results given by Aperathitis et al. [13] under proper experimental conditions.

**2. Analysis**

The schematic diagram of an AlGaAs/GaAs QWSC is shown in Fig.1. Light photons are incident on the ZnS antireflection coating and a part of them transmit into the cell.
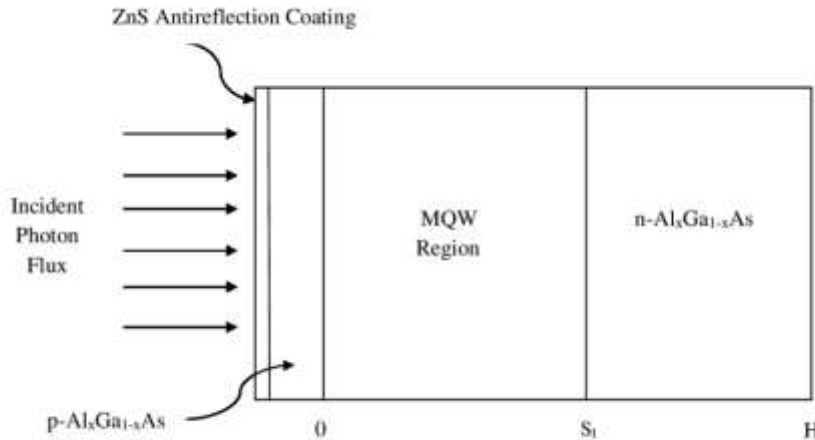


**Fig. 1.** The schematic diagram of a QWSC with ZnS antireflection coating.

Detailed discussion on the tunneling current, thermionic current and the photo-generated current in the base layer has already been presented in [13] and [14]. In both the papers the barriers in the MQW region have been assumed to be rectangular in nature. But, according to Fox et al. [15], the shape of the barrier appears to be trapezoidal in nature and hence the derivation of the tunneling current through the trapezoidal barrier is attempted in this paper. In both the above mentioned papers [13] and [14], it has been assumed that the photons incident on the QWSC totally transmit into the cell. But practically only a part of the incident photons can transmit into the cell and an antireflection coating is required to minimize this reflection loss. Also the reflection coefficient of the total QWSC is dependent on the refractive indices of the anti-reflection coating, the $Al_xGa_{1-x}As$/GaAs MQW region and the p-type front layer region and n-type base regions [16].Therefore, in this paper an analytical

treatment on the tunneling current in the QWSCs has been presented assuming a trapezoidal barrier, and also taking into account the temperature and wavelength dependent refractive indices.

*2.1. Derivation of the expression of the tunneling current density*

The schematic band diagram of an AlGaAs/GaAs QWSC is shown in Fig.2. In the AlGaAs/GaAs QWSC system, intersubband transition of the photo-generated carriers takes place. An electron (or a hole) in the ground state of the quantum well being excited by a photon, transits to the first bound state and readily tunnel out from the well through the barrier, resulting in the tunneling current in the QWSC [17]. An analytical expression of the tunneling current has been derived on the basis of the method described in [13], and subsequently modified by the authors [14].
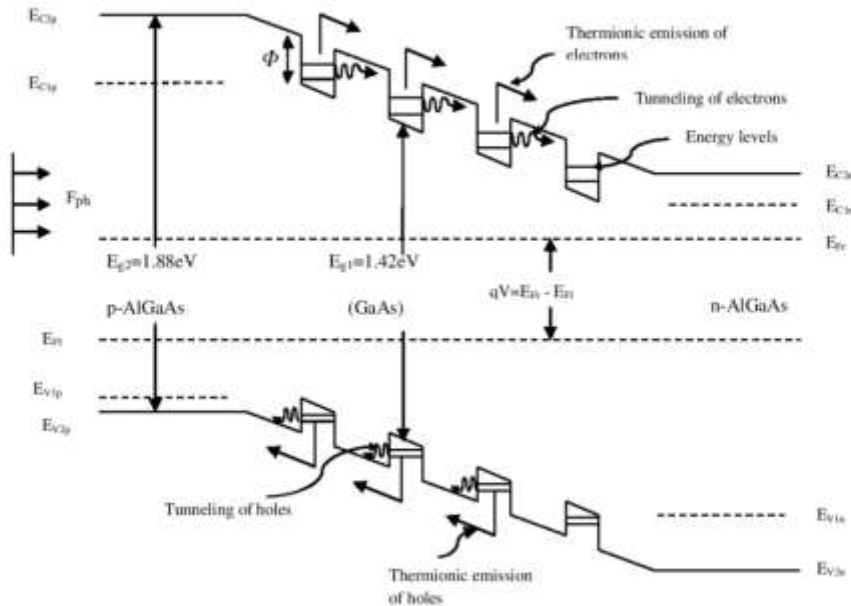
**Fig. 2.** The band diagram of a AlGaAs/GaAs QWSC

The general expression for the tunneling current taking into consideration the electron and the hole flow equations, is as follows [14]

$$I_{TUN} = q\left(\frac{A\tau_T}{S_I}\right)F_{ph}\left(1 - R_c(\lambda)\right)\left(1 - e^{-\alpha(\lambda)s_I}\right)$$

$$\int D(E)T(E)[f(E - qV) - f(E)]v(E)dE \qquad (1)$$

where, q is the electronic charge, A is the cross-sectional area of the QWSC, $\tau_T$ is the carrier transit time for tunneling current for the entire MQW region, $F_{ph}$ is the number of incident photons per cm$^2$ per sec per unit bandwidth, $R_c(\lambda)$ is the reflection coefficient of the entire QWSC, $\alpha(\lambda)$ is the absorption coefficient, $S_I$ is the width of the entire MQW region, $v(E)$ is the velocity of the carriers. The two dimensional density of states D(E) is given by [18],

$$D(E) = \frac{m^*}{\pi\hbar^2} \qquad (2)$$

where, $m^*$ is the effective mass of the carriers.

It may be mentioned here that the barrier in the intrinsic MQW region, through which the electrons (or holes) have to tunnel through, appears to be of trapezoidal nature. In this case the Wentzel-Kramers-Brillouin approximation (the WKB approximation) may be used to obtain the transmission coefficient T(E) of the barrier [19]. For the purpose of computing the transmission coefficient, we consider the barrier to be consisting of a triangular barrier and a trapezoidal barrier, as explained below.

*For Triangular barrier :*

$$T(E) = exp\left[-\frac{4}{3}\frac{S_B\sqrt{2m^*}}{\Phi\hbar}(\Phi - E)^{\frac{3}{2}}\right]$$

$$for \quad \Phi_0 < E < \Phi \qquad (3)$$

*For Trapezoidal barrier :*

$$T(E) = exp\left[-\frac{4}{3}\frac{S_B\sqrt{2m^*}}{\Phi\hbar}\left\{(\Phi - E)^{\frac{3}{2}} - (\Phi_0 - E)^{\frac{3}{2}}\right\}\right]$$

$$for \quad E < \Phi_0 \qquad (4)$$

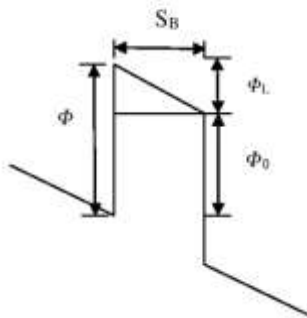where, $S_B$ is the width of the barrier, $\Phi$ is the barrier height.

**Fig. 3.** Schematic diagram of the trapezoidal barrier in the QWSC

The potential $\Phi_0$ may be obtained by writing

$$\Phi_0 = \Phi - \Phi_L \qquad (5)$$

where, $\Phi_L$ may be obtained using simple geometry, as discussed here.
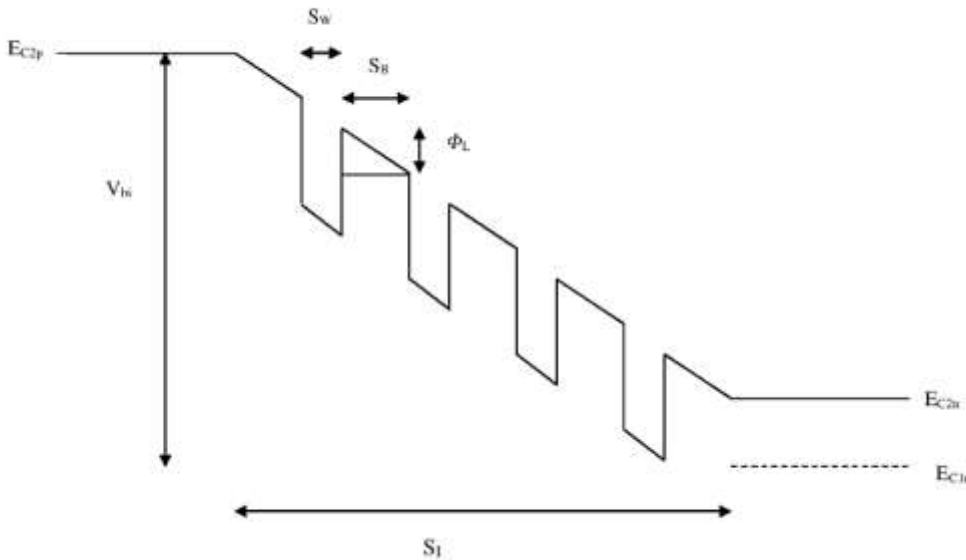


**Fig. 4.** Illustrative form of the conduction band regions of the QWSC

From Fig.4 one can write

$$\Phi_L = \frac{V_{bi}}{S_I} \times S_B \qquad (6)$$

where, $V_{bi}$ is the built-in potential of the device. In analogy with the expression given for the heterojunction solar cells [20], the built-in potential of the QWSC is approximately

$$V_{bi} = E_{g2} + \Delta E_V - (E_{C1n} - E_{Fr}) - (E_{Fl} - E_{V1n}) \qquad (7)$$

where, $E_{g2}$ is the band gap of the barrier material ($Al_xGa_{1-x}As$), $E_{Fr}$ and $E_{Fl}$ are the energy of the quasi-Fermi levels.

$E_{C1n}$ and $E_{V1n}$ are the conduction band energy and the valence band energy of the well material GaAs respectively, near the n-side of the QWSC. The discontinuity in the valence band is $\Delta E_V = (E_{g1} - E_{g2}) - \Delta E_C$, where, $E_{g2}$ and $E_{g1}$ are the band gap energies of AlGaAs and GaAs respectively. The conduction band discontinuity is $\Delta E_C = (\chi_2 - \chi_1)$, where, $\chi_2$ and $\chi_1$ are the electron affinities of AlGaAs and GaAs respectively.

The position of the quasi-Fermi levels $E_{Fr}$ and $E_{Fl}$, can be evaluated using Joyce-Dixon approximation method [19].

The voltage developed across the QWSC has been evaluated using the relation,

$$qV = E_{Fr} - E_{Fl} \tag{8}$$

$$J_{TUN} = q\left(\frac{A\tau_T}{S_I}\right) F_{ph}\left(1 - R_c(\lambda)\right)[1 - exp(-\alpha(\lambda)S_I)]\frac{m^*}{2\pi\hbar^2} sinh\left(\frac{qV}{2kT}\right)$$

Thus assuming trapezoidal potential barrier the tunneling current may be written as,

$$\left[\int_0^{\Phi_0} \frac{\Phi_0 \, exp\left[-\frac{4}{3}\frac{S_B\sqrt{2m^*}}{\Phi\hbar}\left\{(\Phi - E)^{\frac{3}{2}} - (\Phi_0 - E)^{\frac{3}{2}}\right\}\right]\sqrt{\frac{2(\Phi - E)}{m^*}}}{cosh\left(\frac{E - E_{Fl}}{2kT}\right)cosh\left(\frac{E - E_{Fl} - qV}{2kT}\right)} dE + \int_{\Phi_0}^{\Phi} \frac{\Phi \, exp\left[-\frac{4}{3}\frac{S_B\sqrt{2m^*}}{\Phi\hbar}\left\{(\Phi - E)^{\frac{3}{2}}\right\}\right]\sqrt{\frac{2(\Phi - E)}{m^*}}}{cosh\left(\frac{E - E_{Fl}}{2kT}\right)cosh\left(\frac{E - E_{Fl} - qV}{2kT}\right)} dE\right] \tag{9}$$

### 2.2. Equations for thermionic current density and the photo-generated current density in the n-type base region

Another two current densities which appear in QWSC have already been shown by Aperathitis [13] and the authors [14]. These current densities are thermionic current density and the photo-generated current density in the n-type AlGaAs base region.

The equation for the thermionic current density [14] is

$$J_{TH} = q\left(\frac{A\tau_{TH}}{S_I}\right)F_{ph}\left(1 - R_c(\lambda)\right)$$

$$\left(1 - exp\left(-\alpha(\lambda)S_I\right)\right)\frac{\sqrt{2\pi m^*(k)^3}}{2\pi\hbar^2} \times \left(\frac{N_v}{p}\right) \times T^{\frac{3}{2}}$$

$$\times exp\left[-\frac{\delta E_1 + E_{C2n} - E_{v1n} - \Delta_c - qV_1}{kT}\right] \tag{10}$$

where, $\Delta_c$ is the discontinuity in the conduction band, $qV_1$ is the barrier energy, $\delta E_1$ is the energy of the miniband inside the quantum well with respect to the bottom of the well, $E_{C2n}$ is the conduction band energy of AlGaAs near n-side of the QWSC and $\tau_{TH}$ is the transit time for the thermionic current for the entire MQW region.

$$N_v = 2\left(\frac{2\pi m_h^* kT}{h^2}\right)^{\frac{3}{2}} \tag{11}$$

where, $m_h^*$ is the effective mass of holes in GaAs, p is the hole density.

The equation for the photo-generated current density due to the holes in the n-type base region [14] is

$$J_p = \left[\frac{qF_{ph}\left(1 - R_c(\lambda)\right)\alpha(\lambda)L_p}{\left(\alpha^2(\lambda)L_p^2 - 1\right)}\right][exp(-\alpha(\lambda)S_I)]$$

$$\times \left[\alpha(\lambda)L_p - \frac{\left(\frac{SL_p}{D_p}\right)\left[cosh\left(\frac{H'}{L_p}\right) - exp\left(-\alpha(\lambda)H'\right)\right] + sinh\left(\frac{H'}{L_p}\right) + \alpha(\lambda)L_p exp\left(-\alpha(\lambda)H'\right)}{\left(\frac{SL_p}{D_p}\right)sinh\left(\frac{H'}{L_p}\right) + cosh\left(\frac{H'}{L_p}\right)}\right] \tag{12}$$

where, $L_p$ is the diffusion length for holes, $D_p$ is the diffusion coefficient for holes, S is the back surface recombination velocity and $H' = H - S_I$.

As the photo-generated current density due to the p+ AlGaAs front region is very small compared to the total photo-current density, it has been neglected from the analysis.

Thus the total current density for the entire QWSC is

$$J_{TOT} = J_{TUN} + J_{TH} + J_p \qquad (13)$$

### 2.3. Expressions for temperature and wavelength dependent refractive indices

In order to perform the final calculations, in addition to knowing the various device parameters, it is also essential to know the expressions for the refractive indices of the different regions of the QWSC that are dependent on the wavelength of the incident light as well as on the temperature of the device. It is also desirable to know the expressions for the absorption coefficient. All these points are discussed here in brief.

The refractive indices of the main materials of the QWSC i.e. ZnS antireflection coating, AlGaAs barrier layers and the GaAs well layers can mainly depend on the wavelength of the incident light and the temperature. The equations for the temperature and wavelength dependent refractive index of the ZnS have been given in [21]. The wave-length dependent equation of refractive index of GaAs and $Al_xGa_{1-x}As$ is also available in published literature [22].

The temperature dependent relation of the high frequency dielectric constant and refractive index of GaAs has been given in [23].

$$\epsilon_{GaAs} = 10.60(1 + 9.0 \times 10^{-5}T) \qquad (14)$$

$$(\epsilon_{GaAs})^{1/2} = n_{GaAs} = 3.255(1 + 4.5 \times 10^{-5}T) \qquad (15)$$

The variation of the refractive index of AlAs for different temperatures has been measured and a semi-empirical relation between (dn/dt) and t has been discussed [24].

Based on this literature an equation for the high frequency dielectric constant has been found out,

$$\epsilon_{AlAs} = (n_{AlAs})^2$$
$$= 8.630837(1 + 5.105811 \times 10^{-5}t)^2 \qquad (16)$$

where, t is the temperature in $^0C$.

Using the relation given in [25] the values of the high frequency dielectric constant and hence the refractive index of $Al_xGa_{1-x}As$ may be obtained.

$$\epsilon_{Al_xGa_{1-x}As}(x) = (1-x)\epsilon_{GaAs} + x\epsilon_{AlAs} \qquad (17)$$

and

$$n_{Al_xGa_{1-x}As} = \sqrt{\epsilon_{Al_xGa_{1-x}As}(x)} \qquad (18)$$

The refractive index of the total QWSC except the AR layer for normal incidence has been evaluated using the refractive index summation equation [16]. Hence the reflection coefficient of the total QWSC has been found out using Fresnel's equation [16].The equations for the absorption coefficient of GaAs and the $Al_xGa_{1-x}As$ have been obtained from the published literature [19].

### 3. Results and Discussions

Calculations were performed based on the theoretical expressions derived above. Here the incident photon flux has been assumed to be high i.e. $F_{ph} \sim 2.6 \times 10^{16} /cm^2 s$, which is similar to the value considered by Aperathitis [13]. The transit times for tunneling current and thermionic current are considered as $\tau_T \sim 10^{-14} s$ and $\tau_{TH} \sim 10^{-14} s$ respectively. The doping concentration of the p-type (Be-doped) and n-type (Si-doped) $Al_xGa_{1-x}As$ regions are taken as $2 \times 10^{17} cm^{-3}$ and the thicknesses of the two regions are taken 150 nm and 300 nm respectively [13]. The electron effective mass for $Al_xGa_{1-x}As$/GaAs super-lattice is $m_e^* = (0.067 + 0.083x)m_0$ and the hole effective mass for the same is $m_h^* = (0.62 + 0.14x)m_0$, where $m_0$ is the electronic mass and x is taken as 0.36. The band gap of $Al_xGa_{1-x}As$/GaAs is $E_g = (1.426 + 1.247x)eV$. These parameters have been taken from [18]. The energy of the potential barrier has been taken as $qV_1 \sim 0.9eV$ [26]. Electron affinity of $Al_xGa_{1-x}As$/GaAs super-lattice is (4.07-1.1x) eV.

### 3.1. An analytical study on the three current components of QWSC (without antireflection coating) with temperature

For the purpose of calculations, two samples of QWSC have been chosen, as shown in Table 1., whose experimental results for the total photo-current densities for -10$^0$C and 100$^0$C temperatures are known [13].

**Table 1.** Dimensions of the experimental samples given by Aperathitis [13].

| Model | Area of the front surface | Number of wells | Well width | Barrier width | Total width of the MQW region |
|---|---|---|---|---|---|
| Sample 1 | 4.1×10$^{-3}$ cm$^2$ | 23 | 9nm | 6nm | 0.35μm |
| Sample 2 | 2.0×10$^{-3}$ cm$^2$ | 39 | 15nm | 10nm | 0.97μm |

A comparative study has been carried out on QWSC, using trapezoidal barrier model and the experimental results. For these cases the QWSCs were considered to be without antireflection coating.

The variation of tunneling current density, thermionic current density, current density in the n-AlGaAs base region and the total photo-current density for the two samples has been shown in Fig.5, assuming the trapezoidal barrier model.
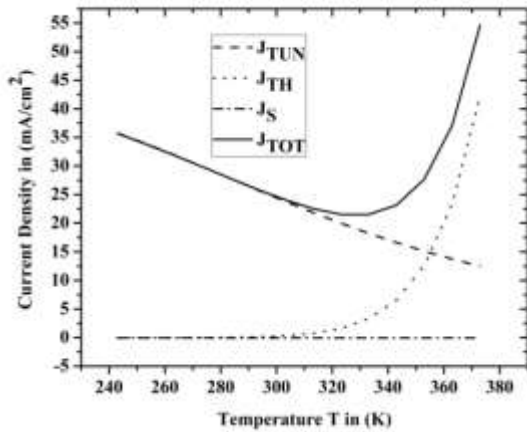


(a)
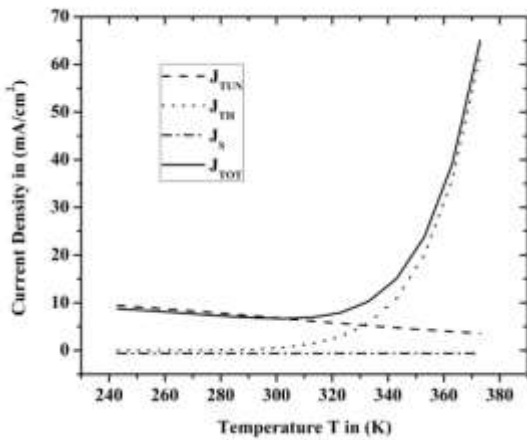


(b)

**Fig. 5. (a)** Variation of the current densities with temperature for Sample 1 assuming trapezoidal barrier model. **(b)** Variation of the current densities with temperature for Sample 2 assuming trapezoidal barrier model.

The comparison of the two theoretical results for the total photo-current density obtained in this work with the experimental results given by Aperathitis [13] has been shown in Table 2.

**Table 2.** The total photo-current densities for the two temperatures

| Model | | Total Current Density | |
|---|---|---|---|
| | | For -10$^0$C | For 100$^0$C |
| Sample 1 | Trapezoidal Barrier Model | 31.95 mA | 54.66 mA |
| | Experimental Results | 31.71 mA | 56.09 mA |
| Sample 2 | Trapezoidal Barrier Model | 7.99 mA | 64.97 mA |
| | Experimental Results | 9.75 mA | 59.26 mA |

From Table 2. it is clearly seen that the analytical results of the total photocurrent densities using trapezoidal barrier model are consistent with the experimental results given by Aperathitis [13].
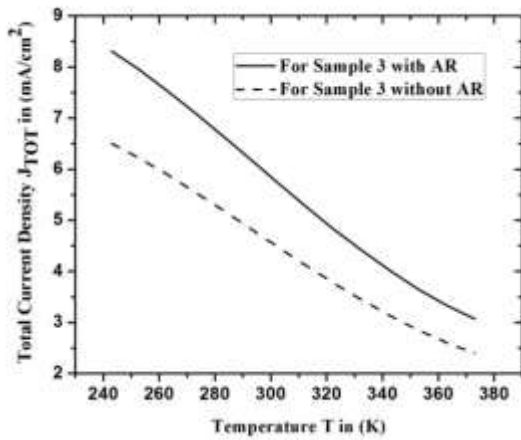
*3.2. A theoretical study on the total photo generated current densities for the QWSCs with and without antireflection coating*

We shall now consider the case when ZnS antireflection coating has been applied to the front surface of the QWSC and will study the results theoretically. For this purpose four samples of QWSC have been considered here, each having different well width and barrier width, which are given in Table 3. In consistence with the previously reported results, the number of wells has been assumed to be 39. The junction area of each QWSC is considered to be $1.0 \times 10^{-3} cm^2$ .

**Table 3.** The values of the well widths and the barrier widths in the intrinsic MQW regions for different samples of AlGaAs/GaAs QWSCs

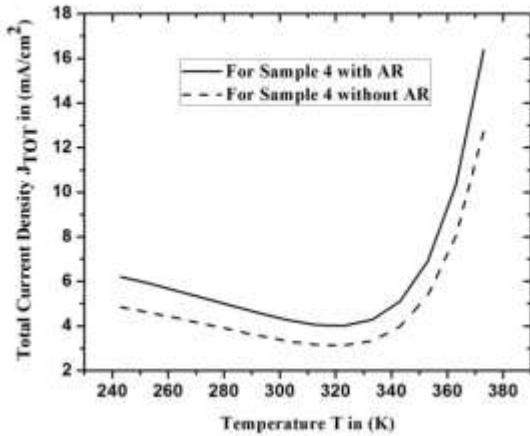| Name of Samples | Well Width in (nm) | Barrier Width in (nm) |
|---|---|---|
| Sample 3 | 5 | 5 |
| Sample 4 | 10 | 10 |
| Sample 5 | 15 | 15 |
| Sample 6 | 20 | 20 |

The variation of the total photocurrent density with temperature for the four samples with and without antireflection coating has been calculated. For this case the wavelength of the incident light has been taken as 650 nm and the composition x=0.36.
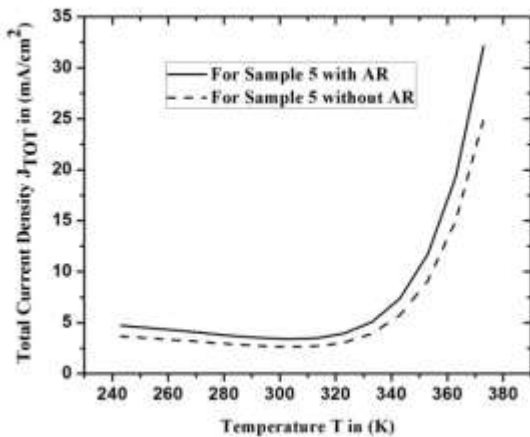
(a)



(b)



(c)



(d)
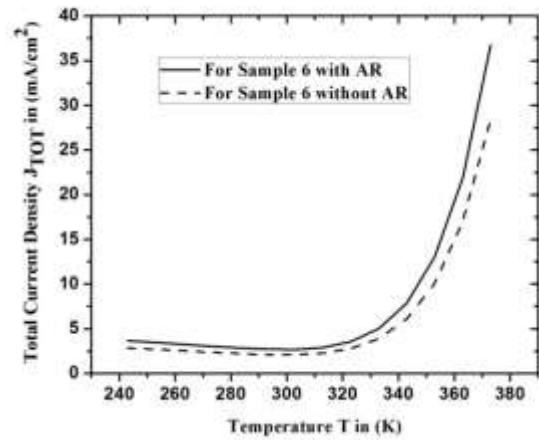
**Fig. 6.** The variation of the total photocurrent density with temperature for the four samples with and without antireflection coating.

From Fig.6. it can be clearly observed that the QWSC having ZnS antireflection coating, gives higher photocurrent density than the cell without antireflection coating. Because the ZnS antireflection coating minimizes the reflection loss of incident photons.

*3.3. Analytical study on the tunneling current density for the QWSCs*

The variations of the tunneling current densities for the four different samples are calculated, with the variation of temperature keeping the wavelength of the incident light as 650nm, x=0.36 and considering ZnS antireflection coating in front of the cell.
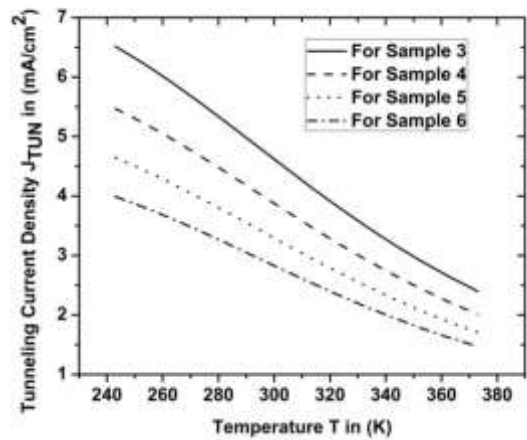


**Fig. 7.** The variation of the tunneling current density with temperature for different samples.

The tunneling current has been plotted as a function of temperature for all the four samples in Fig.7. From the figure it can be observed that the tunneling current decreases with the increase in temperature. It may be due to the fact that with the increase in temperature the occupation probability decreases and consequently the number of available carriers to tunnel through barriers decreases, resulting in a decrease in tunneling current. It is also observed that, the tunneling current density decreases with the increase in barrier-width, which is quite evident.

The variation of tunneling current density for the four samples have been calculated as a function of the wavelength of the incident photon flux at room temperature T=300K and taking x=0.36. The results are shown in Fig.8.
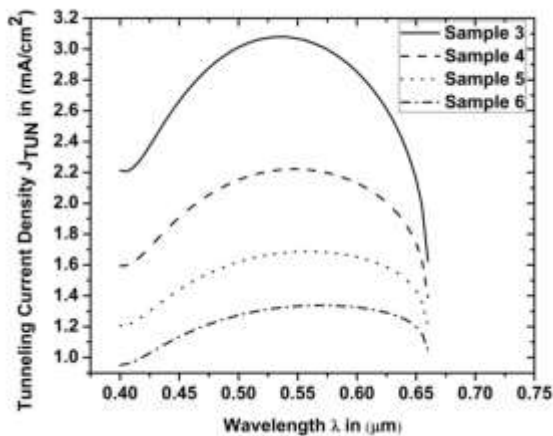


**Fig.8.** The variation of tunneling current density with wavelength of the incident photons for different samples.

It is observed that the tunneling current first increases and then decreases as the wavelength of the incident light increases. For very short values of wavelengths, the tunneling current is small. This may be due to the fact that in the short wavelength region the absorption coefficient is high and in this case most of the carriers are generated near the front ohmic contacts and recombine very quickly before reaching the MQW region. As a result the number of carriers available to tunnel through the barrier decreases, resulting in lower tunneling current density. As the wavelength of the incident photon flux increases, the absorption coefficient of the QWSC decreases and photons corresponding to these larger wavelengths get absorbed in the QWSC. These photons excite the carriers from the lower states to the higher excited states and the carriers can achieve enough energy to tunnel through the barriers, producing higher tunneling current density. But for wavelengths above about 0.55µm, the energy of the incident photons may not be enough to excite the carriers for tunneling. So above this wavelength of

the incident photon flux the tunneling current density gradually decreases.

## 4. Conclusion

The analytical work presented in this paper has been carried out for an AlGaAs/GaAs multiple quantum well solar cell, assuming that the barriers generated in the MQW region are trapezoidal in nature. Results obtained from the above analysis have been shown graphically. The variation of the tunneling current density, thermionic current density and photo-generated current density with temperature has been shown graphically corresponding to two experimental samples. A simple comparison with the theoretical results obtained in this paper has been done with the very few experimental data available in published literature. Here it has been shown that with the introduction of a ZnS antireflection coating in front of the QWSC, the photocurrent density increases in comparison with the case where no anti reflection coating has been added. It is observed that the tunneling current of the QWSC strongly depends on temperature of the cell and on the wavelength of the incident photon flux. With increasing temperature the tunneling current decreases.

## References

[1] U.M. Choi, K.B. Lee and F. Blaabjerg, "Power electronics for renewable energy systems: wind turbine and photovoltaic systems", International conference on renewable energy research and applications (ICRERA), Nagasaki, pp. 1-8, 11-14 November 2012.

[2] Y. Nakanishi, K. Shimazu, Y. Matsumoto, S. Kai, Y. Oka and H. Higaki, "Eco-friendly bearing for tidal power generation", International conference on renewable energy research and applications (ICRERA), Nagasaki, pp. 1-5, 11-14 November 2012.

[3] O. Kaplan, U. Yavanoglu and F. Issi,"Country study on renewable energy sources in Turkey", International conference on renewable energy research and applications (ICRERA), Nagasaki, pp. 1-5, 11-14 November 2012.

[4] E. Barbier, "Geothermal energy technology and current status: an overview", Renewable and Sustainable Energy Reviews. vol. 6, pp. 1-65, 2002.https://doi.org/10.1016/S1364-0321(02)00002-3

[5] J. He, T. Zhao, X. Jing and N.A.O. Demerdash, "Application of wide bandgap devices in renewable energy system-benefits and challenges", 3rd International conference on renewable energy research and applications (ICRERA), Milwakuee USA, pp. 749-754,19-22 October 2014.

[6] L.R.S. Paragond, C.P. Kurian and B.K. Singh, "Design and simulation of solar and wind energy conversion system in isolated mode of operation", 4th International conference on renewable energy research and applications (ICRERA), Palermo Italy, pp. 143-147, 22-25 November 2015.

[7] A. Hemmani, A. Nouri, H. Khachab and T. Atouani, "Optimization of the Emitter's Bandgap and Thickness of AlxGa1-xAs/ GaAs Multi-junction Solar Cell", Int. J. Renewable Energy Research. vol. 7, no. 2, pp. 525-530, 2017.

[8] M.A. Humayun, S. Khan, A.H.M.Z. Alam, M. Yaacob, M. AbdulMalek and M.A. Rashid,"Improvement of Temperature Dependence of Carrier Characteristics of Quantum Dot Solar Cell Using InN Quantum Dot", Int. J. Renewable Energy Research. vol. 7, no. 1, pp. 330-335, 2017.

[9] F. Anwar, S. Afrin, S. S. Satter, R. Mahbub and S. M. Ullah, "Simulation and Performance Study of Nanowire CdS/CdTe Solar Cell", Int. J. Renewable Energy Research. vol. 7, no. 2, pp. 885-893, 2017.

[10] O.Y. Raisky, W.B. Wang and R.R. Alfano, "Resonant enhancement of the photocurrent in multiple-quantum-well photovoltaic devices", Appl. Phys. Lett. vol. 74, no.1, pp. 129-131, Jan 1999. http://dx.doi.org/10.1063/1.122972

[11] K.W.J. Barnham, I. Ballard, J.P. Connoly, N.J. Ekin-Daukes, B.G. Kluftinger, J. Nelson, C. Rohr, "Quantum well solar cells", Physica E. vol. 14, pp. 27-36, 2002. http://dx.doi.org/10.1016/S1386-9477(02)00356-9

[12] O. Jani, C. Honsberg, "Absorption and transport via tunneling in quantum-well solar cells", Sol. Energy Mate. Sol. Cells. vol. 90, pp. 3464-3470, Nov. 2006. http://dx.doi.org/10.1016/j.solmat.2006.01.004

[13] E. Aperathitis, A.C. Varonides, C.G. Scott, D. Sand, V. Foukaraki, M. Androulidaki, Z. Hatzopoulos, P. Panayotatos, "Temperature dependence of photocurrent components on enhanced performance GaAs/AlGaAs multiple quantum well solar cells", Sol. Engergy Mater. Sol. Cells. vol. 70, no.1, pp. 49-69, Dec 2001. http://dx.doi.org/10.1016/S0927-0248(00)00411-6

[14] A. Chatterjee, A. Biswas and A. Sinha, "An analytical study of the various current components of an AlGaAs/GaAs multiple quantum well solar cell", Physica E. vol. 72, pp. 128-133, Aug 2015. http://dx.doi.org/10.1016/j.physe.2015.04.013

[15] A.M. Fox, D.A.B. Miller, G. Livescu, J.E. Cunningham and W.Y. Jan, "Quantum well carrier sweep out: relation to electroabsorption and exciton saturation", IEEE J. Quantum Electronics. vol. 27, no.10, pp. 2281-2294, Oct 1991. 10.1109/3.97272

[16] F.K. Rault, A. Zahedi,"Computational modelling of the reflectivity of AlGaAs/GaAs and SiGe/Si quantum well solar cells", Sol. Energy Mate. Sol. Cells. vol.79, no. 4, pp. 471-484, Sept 2003. http://dx.doi.org/10.1016/S0927-0248(03)00050-3

[17] S.M. Sze and K.K. Ng, Physics of Semiconductor Devices, 3rd ed., Wiley India Pvt. Ltd., 2012, pp. 717.

[18] P. Harrison, Quantum Wells, Wires and Dots, 2nd ed., Wiley-Interscience, John Wiley & Sons, Ltd., 2005, pp. 26, 459-460.

[19] J. Singh, Semiconductor Devices Basic Principles, Wiley India Pvt. Ltd., 2014, pp. 38, 458-463, 515-516.

[20] H.J. Hovel, Semiconductors and Semimetals, Vol. 11, Solar Cells, Academic Press, 1975, pp. 131.

[21] H.H. Li, "Refractive index of ZnS, ZnSe, and ZnTe and its wavelength and temperature derivatives", J. Phys. Chem. Ref. Data. vol. 13, no. 1, pp. 103-150, 1984.http://dx.doi.org/10.1063/1.555705

[22] S. Fara, P. Sterian, L. Fara, M. Iancu and A. Sterian, "New Results in Optical Modelling of Quantum Well Solar Cells", Int. J. Photoenergy. vol. 2012, Art. ID. 810801, pp. 1-9, 2012. http://dx.doi.org/10.1155/2012/810801

[23] J.S. Blakemore, "Semiconducting and other major properties of gallium arsenide", J. Appl. Phys. vol. 53, no.10, pp. R123-R181, Oct 1982. http://dx.doi.org/10.1063/1.331665

[24] J. Talghader and J.S. Smith, "Thermal dependence of the refractive index of GaAs and AlAs measured using semiconductor multilayer optical cavities", Appl. Phys. Letts. vol. 66, no.3, pp. 335-337, Jan 1995. http://dx.doi.org/10.1063/1.114204

[25] S. Adichi, Properties of Aluminium Gallium Arsenide, INSPEC, The Institute of Electrical Engineers, 1993, pp 89-117.

[26] P.H. Holloway, G.E. McGuire, Hand Book of Compound Semiconductors Growth, Processing, Characterization, and Devices, Noyes Publications, 1995, pp. 344.